

System Identification of the Human Hand Grasping a Haptic Knob

Christopher J. Hasser
*Immersion Corporation and
Stanford University*
c.hasser@ieee.org

Mark R. Cutkosky
Stanford University
cutkosky@cdr.stanford.edu

Abstract

Accurate dynamic models of human hands grasping haptic devices can help to inform stability analyses, control algorithms, device design, and technology development efforts. The current study develops and tests a lumped second-order dynamic model for nine subjects holding a haptic knob in a simple pinch grasp. Results include steadily increasing damping and stiffness parameters with increasing grip force, and compare well to the findings of earlier investigators. Moment of inertia estimates, expected to remain constant, dropped for very large grip forces, illustrating limitations in the second-order model.

1. Introduction

Haptic designers and researchers have long known that the stability of haptic interfaces depends heavily on the biomechanical properties of users' hands. The size of the hand, the strength of the grasp, and other factors can lead to wide variations in stability. A device that remains stable when held in a moderate to strong grip may begin to chatter when held in a light grip. In order to design haptic devices for inherent stability (e.g. specifying mechanical parameters, determining acceptable sensor or actuator quantization, etc.), or to implement stability-enhancing control schemes, one needs to know the range of mechanical system properties that a user's hand could present to the system.

Questions such as the determination of adequate encoder resolution can have a bearing on the quality of fielded products, and can also help to guide strategic technology development decisions. Technology development efforts should be motivated by specific requirements intended to meet a demonstrated need. Stability-enhancing algorithms can increase the quality of haptic interfaces and may allow quality to remain constant while designers reduce system costs. Accurate models of the human hand in a knob grasp would help towards these ends, and would also provide a valuable simulation tool for testing designs. The present work develops lumped second-order dynamic models of the human hand grasping a 17.8 mm diameter haptic knob in a simple pinch grasp.

2. Related Work

Previous studies of human dynamics have reported wide intersubject variability. This corresponds to the haptics engineer's intuition that devices that appear stable with one individual may appear stable with another individual, or unstable at different frequencies. Kearney studied human ankle dynamics, reporting that inertia, elasticity, and the slope of the linear relation between torque and K had an intersubject coefficient of variation between 30% and 50% [Kearney et al., as cited in Kearney and Hunter 1990, ref. 137]. Interestingly, there was substantially less variability in the damping parameter, with an intersubject coefficient of variation of only 15%. Kearney and Hunter used a test-retest paradigm for their study, and reported excellent intrasubject repeatability.

Many sources have supported the validity of modeling human joint dynamics as linear about an operating point, with second-order models being common [Agarwal and Gottlieb, 1977; Becker and Mote, 1990; Crowninshield et al., 1976; Gillespie et al., 1999; Hogan, 1990; Hunter and Kearney, 1982; Kearney and Hunter, 1982, 1983, 1990; Kearney et al., 1997; Milner and Franklin, 1995, 1998]. Most modeling approaches assume a time-invariant system – expanding the scope to include time-varying behavior greatly increases model complexity and the repeatability challenge. For a human hand in a haptic knob grasp, this implies that the grip remains constant, motion about the origin is small to avoid changing kinematics, and muscle activation does not change to affect the stiffness or damping characteristics of the grasp.

The potential for changes in muscle activation raises some challenges to time-invariance. Muscle stretch reflex responses can be seen in EMG signals from the hand muscles in as little as 20-30 ms [Milner and Franklin, 1995]. By comparison, muscle stretch reflexes for the ankle have been shown to have a minimum latency of 40 ms [Kearney et al., 1997]. Cutaneous slip reflexes can occur in fingers grasping an object at about 70 ms after onset of slip [Johansson and Westling, 1984]. Voluntary muscle activation occurs at longer latencies. One strategy to avoid the complication

of changes in muscle activation is to apply and remove input stimuli rapidly, before any voluntary or reflexive muscle activation can occur [Hajian, 1997; Kearney and Hunter, 1990; others].

2.1. Previous Studies of Finger Dynamics

Several studies have been conducted on the dynamic properties of the human finger. Hajian conducted the study most relevant to the current work. A thorough description of Hajian's work appears below. Becker and Mote [1990] studied the dynamics of the index finger in abduction/adduction, finding that a second order mass-spring-damper model described the dynamics well for small displacements, and that fatigue of the finger muscles reduced the stiffness and damping parameters. Milner has conducted studies on fingers specifically motivated by haptic feedback applications [Milner and Franklin, 1995, 1998]. Karason and Srinivasan [1995] studied finger dynamics in a grasp of an active instrumented object that could rapidly contract or expand, deriving a third-order model with separate terms for the finger impedance and fingerpad impedance. Gulati studied the *in vivo* compressibility of the human fingerpad [Gulati, 1995; Gulati and Srinivasan, 1995; Srinivasan et al., 1992]. Further work in the same laboratory has examined the viscoelastic properties of the fingerpad [Birch and Srinivasan, 1999]. Pawluk and Howe have also investigated the dynamics of the fingerpad in compression [Pawluk and Howe, 1999a,b].

Hajian conducted an extensive study of the impedance of the human fingers [Hajian, 1997]. He began with an investigation of the impedance of the straightened index finger in extension and abduction at the metacarpal-phalangeal (MCP) joint, continued with an investigation of the impedance of a pinch grasp, built on these results to present and validate a model of the human hand in a drum roll on a musical drum, and finished with an implementation of robotic drumming. Hajian showed that drummers are able to overcome bandwidth limitations on active control by modulating their passive impedance, creating drum rolls at a higher frequency than they could control actively.

In his first study examining the impedance of the index finger MCP joint in extension and abduction, Hajian used transient forces with a maximum duration of 20 milliseconds to avoid the onset of the stretch reflex at approximately 30 milliseconds, and to avoid cutaneous slip reflex [Johansson and Westling, 1984] and voluntary muscle contraction. He used five subjects holding a rigid handle and extending their finger over a pneumatic piston with a force sensor and piezoelectric accelerometer. The subjects began slowly pressing against the piston, and at a force level set by the experimenter (between 2 N and 20 N), the piston would

apply a transient force displacing the finger approximately 5 mm.

Hajian assumed a linear, second-order translational model at the fingertip, with parameters m , b , and k :

$$m\mathbf{x}''(t) + b\mathbf{x}'(t) + k\mathbf{x}(t) = \mathbf{f}(t)$$

Hajian measured applied force and finger tip acceleration just prior to expansion of the cylinder, and calculated velocity and displacement curves from the acceleration signal. Writing the above equation in matrix form allowed Hajian to divide the position, velocity, and acceleration matrix by the force vector to obtain the m , b , k parameter vector (using the matrix division function in MATLAB gives a least-squares fit). Results showed increasing damping and stiffness parameters for all subjects with increasing finger bias force – as subjects pressed harder against the plate, their fingers exhibited more damping and stiffness.

Hajian's second study measured variations in finger impedance in a pinch grasp of a freely supported rigid object. He computed a separate second-order lumped parameter model for each finger in a manner similar to that of the first experiment, with similar results. Mass estimates for subjects' thumbs and forefingers did not vary significantly over the range of finger grasp forces and palm grasp forces. Both damping and stiffness increased almost linearly with finger grasp force. Hajian found that damping and stiffness estimates increased slightly with increasing palm grip force, implying that cocontraction of the muscles in or near the thumb and forefinger was contributing to stiffness and damping.

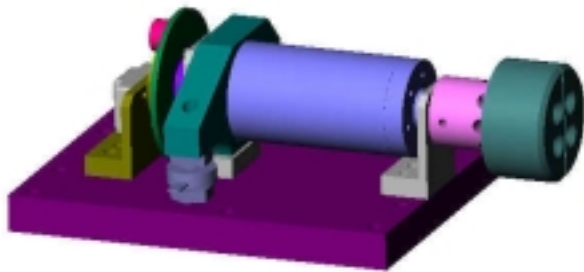
2.2. Hardware Setup

Investigating the dynamics of the human hand grasping a haptic knob requires a testbed with a high-fidelity torque actuator having as little friction and inertia as possible. A position sensor should have high enough resolution to give excellent velocity signals and to far exceed the resolution available on commercial haptic knobs (currently in the range of 4,000 optical encoder counts per revolution, after quadrature). Direct measurement of rotational acceleration would be beneficial (but was not implemented for the current work).

To meet these requirements, a haptic knob reference system dubbed "HREF" was designed and built (see Acknowledgements for design team credits). Figure 1 shows a 3D CAD drawing of the system (with a 29 mm knob cap not used in the current experiments). The illustration includes a reaction torque load cell in the center foreground that was tested with the system, though off-axis moments on the load cell prevented reliable torque measurements during the present experiments. HREF uses a Maxon RE025-118752 motor, similar to those used on haptic feedback interfaces from

Immersion Corporation and SensAble Technologies. A TA-115 transconductance amplifier from Trust Automation, San Luis Obispo, CA, drives the RE025 motor. One D/A channel of a National Instruments 6052E PCI I/O card drives the command input of the TA115 motor amplifier.

HREF possesses a 640,000 count per revolution reflective-diffraction “Mercury” optical encoder from MicroE Systems Corporation [MicroE, 2001]. The HREF design has provisions for a disk mounted on the motor shaft to carry a small accelerometer near the outer edge of the disk with the measurement axis aligned tangent to the disk (using a linear accelerometer to measure angular acceleration), though this feature has not been implemented. Other measurement capabilities include knob torque sensing and the “squeeze” force of the human subject’s grip on the knob. The latter has been implemented for several different-sized knobs, using an Entran EFLS-B1 100 N (22.5 lb) button-style compression load cell amplified by an Entran PS30A amplifier with outputs connected to differential A/D inputs on a National Instruments 6052E I/O card.



Design and drawing: B. Schena

Figure 1: Haptic Reference (HREF) knob apparatus

2.3. Software Architecture

Two computers were used during data collection for all experiments. A host computer ran a Matlab shell program under a Windows operating system, and a target computer ran a real-time executable program over a real-time operating system kernel provided as part of the Mathworks Real-Time Workshop xPC Target system. The target executable began before run-time as a Simulink model program on the host, and was compiled for the target and downloaded to the target over a TCP/IP connection.

The target PC contained the National Instruments 6052E interface card with differential A/D lines for reading the torque and grip load cells, and D/A for outputting command signals to the motor amplifier. The target PC also contained a CIO-QUAD04 board from Measurement Computing, Inc. (formerly ComputerBoards) for reading quadrature encoder signals from the optical encoder rotation sensor on HREF. The target program ran for the duration of a

block of trials, reading sensors and commanding motor torque at a rate of 10 kHz, with periodic parameter updates over TCP/IP from the host computer running the Matlab shell program to cycle through experimental conditions (grip force threshold, pulse strength, etc.). A state-machine running on the target system sensed grip threshold and determined when to fire a pulse, with parameters set by the host. During conduct of a block of experimental trials, data was automatically uploaded to the host after each pulse to be stored for later analysis. The shell program on the host also displayed the data to the experimenter as each pulse occurred to ensure that data collection was proceeding without complication.

3. System Identification for a Fingertip Pinch Grasp

3.1. Introduction

Dynamics for a hand grasping a knob will vary considerably from user to user, for various grasp postures, with different grip strengths, and potentially with other variables. This paper describes system identification of the human hand in a fingertip pinch grasp, with the thumb and forefinger in opposition, pinching the knob, as in Figure 2.

3.2. Methods

3.2.1. Experimental Procedure

Nine healthy subjects between the ages of 23 and 32 participated; five male and four female. For each trial, an audible “beep” signaled subjects to start slowly squeezing the knob in a pinch grasp. When the subject’s grip strength reached a preset threshold for a given trial, the HREF knob applied a 20 ms clockwise torque pulse to the subject’s hand, displacing it approximately 0.07 – 0.11 radians. The subject then relaxed his or her hand to a preset level and awaited the next “beep” from the computer. Pulse magnitudes were increased with increasing grip strengths so that the rotational displacement of the knob remained roughly the same across trials for different grip strengths.

Subjects completed the tests in blocks of 18 trials, with three trials in each block for each of six grip strengths: 0.72, 1.3, 2.4, 4.3, 7.8, and 14.2 Newtons. The trials in each block were presented sequentially, starting with three trials at the lightest grip strength and progressing to three trials at the strongest grip strength. Subjects completed one training block of trials, and three experimental blocks for which data was analyzed.

Prior to beginning the training block, subjects were instructed to assume a neutral and relaxed posture, with chair height adjusted so that the right forearm remained close to level, and the fingers of the right hand grasping

the knob in the pinch grasp illustrated in Figure 2. Subjects were asked not to allow their hand or arm to touch the laboratory table top upon which the knob rested, and to avoid significant extension or flexion of their wrists. Subjects grasped the knob with fingerpads centered on red tape strips indicating the center of the grip force load cell, and kept their fingers as close as possible to directly opposite each other along an axis passing through the center of the load cell. The desired grasp posture was designed to be realistic, repeatable, and to keep the grasp axis passing through the grip load cell for accurate grip force measurement. Subjects were coached on grasp posture during the training block of trials, and subjects did not have trouble maintaining a grasp that appeared satisfactory to visual inspection throughout the blocks of trials. Subjects were instructed to keep their grasp as constant as possible through a given block of trials, but were encouraged to let go of the knob and move freely to relax between blocks.

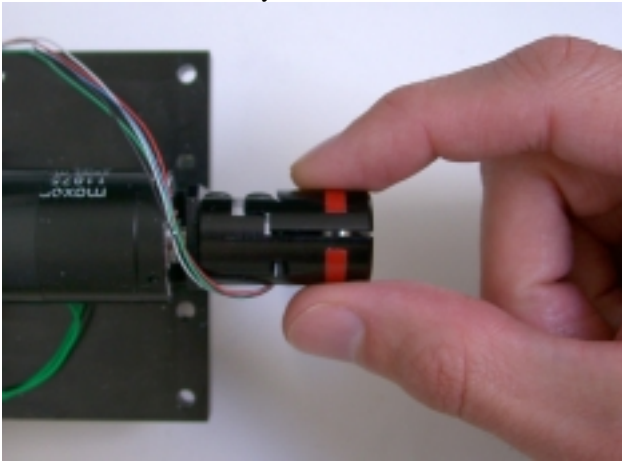


Figure 2: Subject's hand grasping HREF knob in a pinch grasp.

3.2.2. System Identification Technique

This experiment uses similar assumptions and technique to that of Hajian [Hajian, 1997]. It assumes a linear, second-order rotational model at the fingertip, with parameters J , B , and K representing the moment of inertia, damping coefficient, and stiffness coefficient, respectively:

$$J\theta''(t) + B\theta'(t) + K\theta(t) = \mathbf{T}(t)$$

Figure 4 contains a schematic representation of the lumped second-order model:

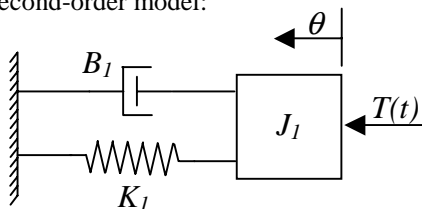


Figure 3: Second-order lumped parameter model

The experimental apparatus collected raw data for knob position, commanded torque, reactive torque measurement, and grip force measurement. Estimates of velocity and acceleration were obtained by differentiation, and double differentiation, respectively, of the rotational position signal. Prior to differentiation, raw displacement data was averaged for all trials for the same condition in a block. The position and velocity signals were smoothed by filtered decimation and interpolation. The high sample rate (10,000 samples/second), extremely high encoder resolution (640,000 counts/revolution) and relatively noiseless encoder signal made double differentiation a viable approach. Writing the above equation in matrix form allows division of the rotational position, velocity, and acceleration matrix by the torque vector to obtain the J , B , K parameter vector (using the matrix division function in MATLAB gives a least-squares fit). Since data was captured for both commanded torque and measured torque, either data vector could be used in the estimation of J , B , and K .

3.3. Results

Figure 4 contains a composite plot showing commanded torque (upper left), acceleration (upper right), velocity (lower left), and position (lower right) vectors for a typical trial. The onset of the pulse causes a sharp acceleration pulse, with steadily ramping velocity and increasing position displacement. Figure 5 contains a plot of commanded torque, estimated torque contributions from moment of inertia, damping, and displacement, as well as total estimated torque. The estimated inertial, damping, and stiffness torques represent the product terms on the left-hand side of the equation:

$$J\theta''(t) + B\theta'(t) + K\theta(t) = \mathbf{T}(t)$$

obtained by multiplying estimated J , B , and K parameters by the acceleration, velocity, and displacement trajectories, respectively. For a perfect model estimate, the estimated inertial, damping, and stiffness torque contributions would add to create a total estimated torque vector that equals the commanded torque.

Figure 6 through Figure 9 show the results of the experiment. Figure 6 shows measured step responses for six different grip forces in a given trial (solid lines), simulated trajectories based on model estimates derived from the same data (dotted lines), and simulated trajectories based on models derived using data from a different trial (dot-dashed lines). This example shows excellent agreement between the data and a model based on the data, and good agreement between the data and a second model estimate based on different data from the same subject under the same conditions.

Figure 7 shows moment of inertia, damping, stiffness, and damping ratio estimates for one subject across all three blocks of trials, for all six grip strengths. The equation $\zeta = B / 2\sqrt{JK}$ defines the damping ratio for the system. Error bars indicate standard deviation across the three blocks of trials. Figure 8 presents moment of inertia, damping, stiffness, and damping ratio estimates for all nine subjects. These plots for all subjects reveal quite similar trend behavior for each parameter. Figure 9 contains plots of moment of inertia, damping, stiffness, and damping ratio estimates averaged across all subjects, with error bars indicating standard deviations. All plots in the three previous figures include the lumped parameter estimates for the combined hand-apparatus system. Apparatus dynamics were empirically determined using torque pulses similar to those used in the human experiments. Stiffness and damping inherent in the HREF apparatus were negligible. A moment of inertia of 19.8 gm-cm² was determined for the apparatus.

Between-subjects coefficients of variation were calculated using the data presented in Figure 9, and the coefficient of variation equation:

$$CV = \frac{\sigma}{\mu},$$

where σ represents the standard deviation of the parameter estimates across subjects for a particular grip force, and μ represents the mean parameter value across subjects for a particular grip force. Coefficients of variation for moment of inertia ranged from 4% to 10% (though since moment of inertia is dominated by the apparatus, this represents a much larger percentage of the finger inertia). Coefficient of variation for damping ranged from 9% to 19%. Coefficient of variation for stiffness ranged from 19% to 48%. Coefficient of variation for damping ratio ranged from 5% to 19%.

3.4. Discussion

Results for damping and stiffness match the experience of haptic researchers and designers – increasing grip strength increases stiffness and damping. The nearly linear increase in damping and stiffness with increasing grip force compares well to results of other researchers [e.g. Hunter and Kearney, 1982, 1983; Kearney and Hunter, 1982; Hajian, 1997]. This behavior allows one to eliminate some unwanted vibrations in a haptic system by gripping the manipulandum with a stronger grip, and makes a light grasp the preferred grasp of persons attempting to excite “buzzing” limit cycles in a haptic system. In fact, a common approach to excite limit cycles with some mechanisms (such as a two-dimensional pantograph) is to tilt them slightly so that the manipulandum moves

with a small force against a virtual wall, with absolutely no additional damping or stiffness from a human grasp. The parameter estimates presented in this work may be useful to haptic designers seeking to simulate new system configurations with the inclusion of a “virtual human” in the simulation.

Moment of inertia should remain constant for each subject across all grip strengths, though it appears to decrease significantly with increasing grip strengths. Hajian found that changes in finger posture with increasing force led to differences in estimated inertia for the finger in extension [Hajian, 1997]; however, differences in grasp posture were not observed as grip force increased. Consideration of a fourth order system consisting of two cascaded second order systems for the finger and for the fingerpad/apparatus provides a possible explanation for the decreasing moment of inertia estimates observed with increasing grip force. In work omitted here for brevity, simulations confirmed this cascaded fourth-order model as a plausible explanation.

Damping ratio estimates for the current experiment reveal underdamped behavior in almost every case, with the damping ratio approaching 1.0 only for the strongest grip forces. Knob rotation for the simple pinch grasp studied here primarily involves finger abduction/adduction. Two studies of finger abduction/adduction dynamics show underdamped behavior to be more likely for this case [Becker and Mote, 1990; Hajian, 1997]. These observations for abduction/adduction are consistent with the results of the current experiment. The underdamped behavior for abduction/adduction and knob rotation with a pinch grasp differ from findings for other situations such as finger flexion/extension, where the behavior is more likely to be overdamped or close to critically damped [Hajian, 1997].

Intrasubject variability for all four parameters was moderate, as was intersubject variability. Data from all subjects showed similar trends for each of the four parameters with changes in grip force. Data from all subjects indicates a significantly underdamped system for all but the strongest grip force. Subjects commented that this grip force was much stronger than they would typically use to grasp a knob (they also commented that the lowest grip force was much lighter than they would use in practice). The underdamped system estimates contrast with the results of Hajian (1997), whose subjects were more likely to exhibit close to critically damped behavior for finger extension experiments.

The results presented here are valid for the specific displacement magnitudes that occurred during this experiment. Isolated muscle typically exhibits higher stiffness when subjected to small displacements than when subjected to large displacements, and one study

found significant decreases in ankle stiffness for larger displacements (Kearney and Hunter, 1982).

The sequential ordering of grip force conditions during data collection for this experiment, from lightest grip to strongest grip in each block, raises a question about the potential for muscle fatigue to introduce systematic artifacts into the data. This concern is mitigated by the fact that a block of trials typically lasted only 3-4 minutes, and was accompanied by a 1-2 minute rest before the next trial. A previous study found that fatiguing of the ankle for as long as 80 seconds did not alter ankle dynamics [Hunter and Kearney, 1983]. A study of fatigue effects on finger abduction/adduction dynamics (quite relevant to the current experiment) showed significant fatigue effects; in the fatigued case, finger stiffness and damping decreased markedly, reducing the frequency and increasing the magnitude of the second order system's resonant peak [Becker and Mote, 1990]. That fatigue study used two exercises to fatigue the finger: 1) repeated lifting of a 5.88 N (1.32 N) weight 75 times with the palmar interosseus muscle and then 75 times with the dorsal interosseus muscle, and 2) maintaining a maximum voluntary isometric contraction for one minute. Each of these exercises is much more strenuous than the short, intermittent squeezes required of subjects in the current experiment.

3.5. Conclusions

Results show that for light to moderate grip forces, a second order linear lumped parameter model provides an excellent estimate of the dynamics of a human hand grasping a knob. Both intersubject and intrasubject variability are nontrivial, but compatible with reliable estimates of human grasp dynamics. Stronger grip forces challenged the second order model assumption. A higher order model that treats finger impedance and fingerpad impedance separately provides a substantially better explanation of combined system behavior. The system models provided here should provide a useful starting point for simulations of haptic knob systems grasped by hands.

4. Acknowledgements

Bruce Schena of Immersion Corporation led the design and construction of the HREF system. Oliver Astley and Danny Grant, also of Immersion, contributed to the design. Prof. Chris Gerdes of Stanford gave valuable guidance and encouragement for the system identification experiments. Several other Immersion employees and Stanford students gave advice on programming and system architecture issues. Many members of the haptics community graciously made themselves available for consultation by phone and e-mail.

5. References

- G. C. Agarwal and G. L. Gottlieb, "Compliance of the human ankle joint," *ASME Journal of Biomechanical Engineering*, Vol. 99, pp. 166-170, 1977.
- J. D. Becker and C. D. Mote Jr., "Identification of a frequency response model of joint rotation," *Journal of Biomechanical Engineering*, Vol. 112, pp. 1-8, 1990.
- A. S. Birch, "Experimental Determination of the Viscoelastic Properties of the Human Fingerpad," S.M. thesis, MIT, Cambridge, MA, 1998.
- R. Crowninshield, M. H. Pope, R. Johnson, and R. Miller, "The impedance of the human knee," *Journal of Biomechanics*, Vol. 9, No. 8, pp. 529-535, 1976.
- J. M. Dolan, M. B. Friedman, and M. L. Nagurka, "Dynamic and Loaded Impedance Components in the Maintenance of Human Arm Posture," *IEEE Transactions on Systems, Man, and Cybernetics*, Vol. 23, No. 3, pp. 698-709, May/June 1993.
- B. Gillespie, P. Tang, and C. Hasser, "Cancellation of Feedthrough Dynamics Using a Force-Reflecting Joystick," *ASME International Mechanical Engineering Conference and Exposition*, Nashville, TN, November 1999.
- B. Gillespie and M. Cutkosky, "Stable User-Specific Rendering of the Virtual Wall," *Proceedings of the ASME International Mechanical Engineering Conference and Exposition*, DSC-Vol. 58, Atlanta, GA, Nov 17-22, 1996. pp. 397-406.
- R. J. Gulati, "Determination of mechanical properties of the human fingerpad, in vivo, using a tactile stimulator," MS thesis, Boston University, Boston, MA, 1995.
- R. J. Gulati and M. A. Srinivasan, Human fingerpad under indentation I: static and dynamic force response, *Proceedings of the 1995 Bioengineering Conference*, Eds: R. M.
- A. Z. Hajian, "A Characterization of the Mechanical Impedance of Human Hands," Ph.D. dissertation, Harvard University, September, 1997.
- A. Z. Hajian and R. D. Howe, "Identification of the mechanical impedance at the human finger tip," *International Mechanical Engineering Congress, American Society of Mechanical Engineers*, Chicago, IL, November 1994, *Proceedings ed. C. J. Radcliffe*, DSC-vol. 55-1, p. 319-327.
- A. Z. Hajian, D. S. Sanchez, and R. D. Howe, "Drum Roll: Increasing Bandwidth Through Passive Impedance Modulation," *IEEE Int. Conf. On Robotics and Automation*, Albuquerque, NM, April 1997.

- N. Hogan, "Mechanical Impedance of Single- and Multi-Articular Systems," *Multiple Muscle Systems: Biomechanics and Movement Organization*, Chapter 9, J. M. Winters and S. L-Y. Woo (ed.), Springer-Verlag, New York, 1990.
- I. W. Hunter and R. E. Kearney, "Dynamics of Human Ankle Stiffness: Variation with Mean Ankle Torque," *Journal of Biomechanics*, Vol. 15, No. 10, pp. 747-752, 1982.
- I. W. Hunter and R. E. Kearney, "Invariance of ankle dynamic stiffness during fatiguing muscle contractions," *Journal of Biomechanics*, Vol. 16, No. 12, pp. 985-991, 1983.
- R. Johansson and G. Westling, "Roles of glabrous skin receptors and sensorimotor memory in automatic control of precision grip when lifting rougher or more slippery objects," *Experimental Brain Research*, Vol. 56, pp. 550-564, 1984.
- S. Karason and M. A. Srinivasan, "Passive human grasp control of an active instrumented object," *Proceedings of the International Mechanical Engineering Congress and Exposition*, ASME, Chicago, IL, DSC Vol. 57-2, pp. 641-647, November, 1995.
- R. E. Kearney and I. W. Hunter, "Dynamics of human ankle stiffness: Variation with displacement amplitude," *Journal of Biomechanics*, Vol. 15, No. 10, pp. 753-756, 1982.
- R. E. Kearney and I. W. Hunter, "System Identification of Human Joint Dynamics," *Critical Reviews in Biomedical Engineering*, Vol. 18, Issue 1, pp. 55-87, 1990.
- R. E. Kearney, R. B. Stein, and L. Parameswaran, "Identification of intrinsic and reflex contributions to human ankle stiffness dynamics," *IEEE Trans. on Biomedical Engineering*, Vol. 44, No. 6, pp. 493-504, 1997.
- K. E. MacLean, C. J. Hasser, and L. Chu, "Driving with Programmable Haptic Feedback: Design Scenarios and Contextual Evaluation," *in review*.
- MicroE Systems Corporation, corporate literature, <http://www.microsys.com>, Natick, MA, 2001.
- Pawluk, D.T.V. and Howe, R.D. Dynamic Lumped Element Response of the Human Fingerpad, *ASME Journal of Biomechanical Engineering* 121(2):178- 184, April 1999.
- Pawluk, D.T.V. and Howe, R.D. Dynamic contact of the human fingerpad against a flat surface, *ASME Journal of Biomechanical Engineering* 121(6):605-611, December 1999.
- T. E. Milner and D. W. Franklin, "Two-dimensional endpoint stiffness of human fingers for flexor and extensor loads," *Proceedings of the International Mechanical Engineering Congress and Exposition*, ASME, Chicago, IL, DSC Vol. 57-2, pp. 649-656, November, 1995.
- T. E. Milner and D. W. Franklin, "Characterization of Multijoint Finger Stiffness: Dependence on Finger Posture and Force Direction," *IEEE Transactions on Biomedical Engineering*, Vol. 45, No. 11, pp. 1363-1375, 1998.
- B. M. Schena, personal communication, August 2001.
- SolidWorks Corporation, <http://www.solidworks.com>, 300 Baker Avenue - Concord, MA 01742, August 2001.
- M. A. Srinivasan, R. J. Gulati, and K. Dandekar, In vivo compressibility of the human fingertip, *Advances in Bioengineering*, Ed. M.W. Bidez, ASME Winter Annual Meeting, November 1992.
- Trust Automation, San Luis Obispo, CA, personal communication, July 2001.
- F. E. Zajac and J. M. Winters, "Modeling Musculoskeletal Movement Systems: Joint and Body Segmental Dynamics, Musculoskeletal Actuation, and Neuromuscular Control," *Multiple Muscle Systems: Biomechanics and Movement Organization*, Chapter 8, J. M. Winters and S. L-Y. Woo (ed.), Springer-Verlag, New York, 1990.
- R. E. Ellis, N. Sarkar, and M. A. Jenkins, "Numerical Methods for the Force Reflection of Contact," *ASME Trans. On Dynamic Systems, Modeling, and Control* 119(4):768-774, 1997.

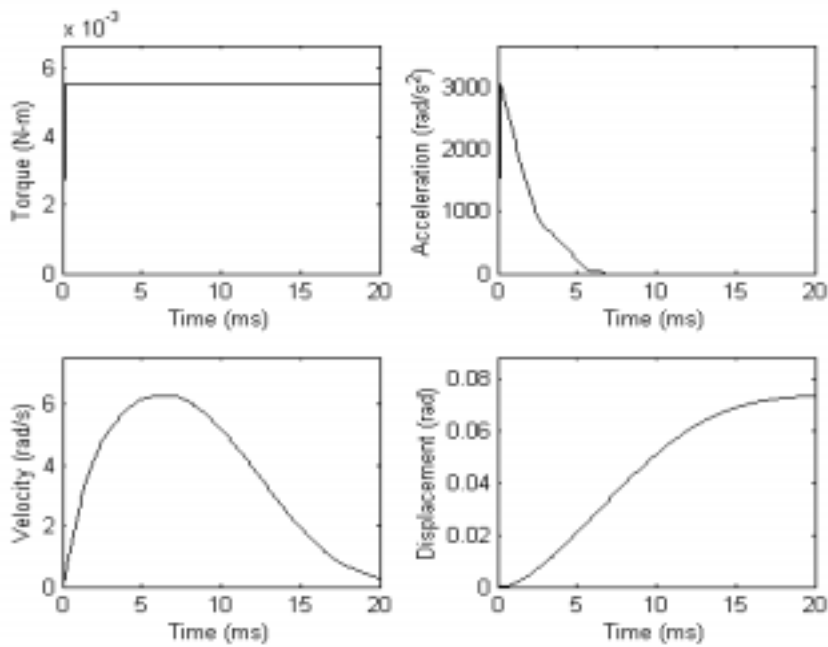


Figure 4: Commanded torque (upper left), acceleration (upper right), velocity (lower left), and displacement vectors (lower right) for a typical trial with a grip force of 2.4 N.

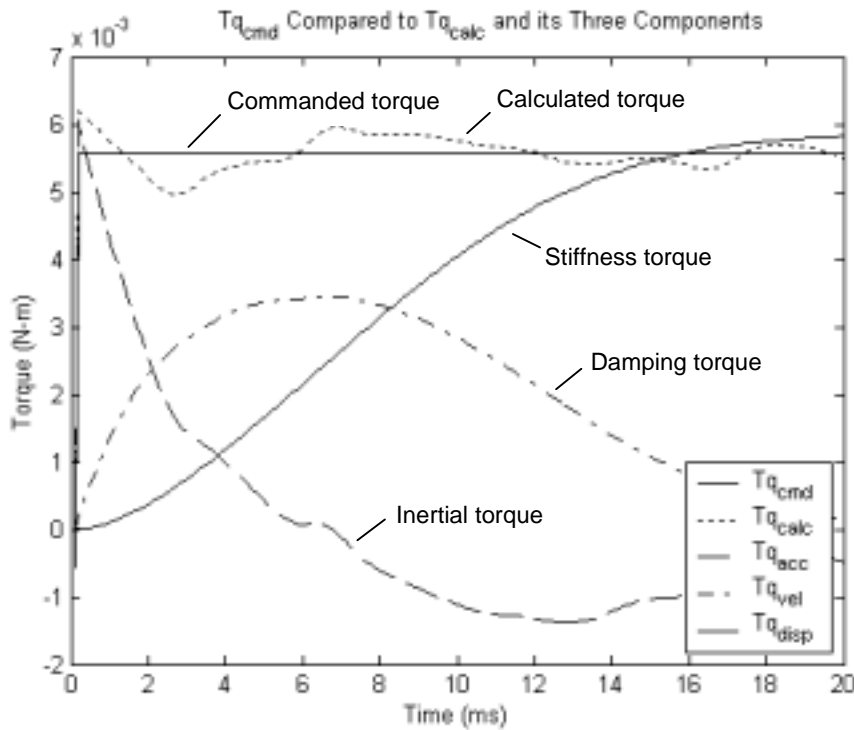


Figure 5: Commanded torque ($T_{q_{cmd}}$), total estimated torque ($T_{q_{calc}}$), and estimated torque contributions from moment of inertia ($T_{q_{acc}}$), damping ($T_{q_{vel}}$), and displacement ($T_{q_{disp}}$) [plot layout adapted from Hajian, 1997].

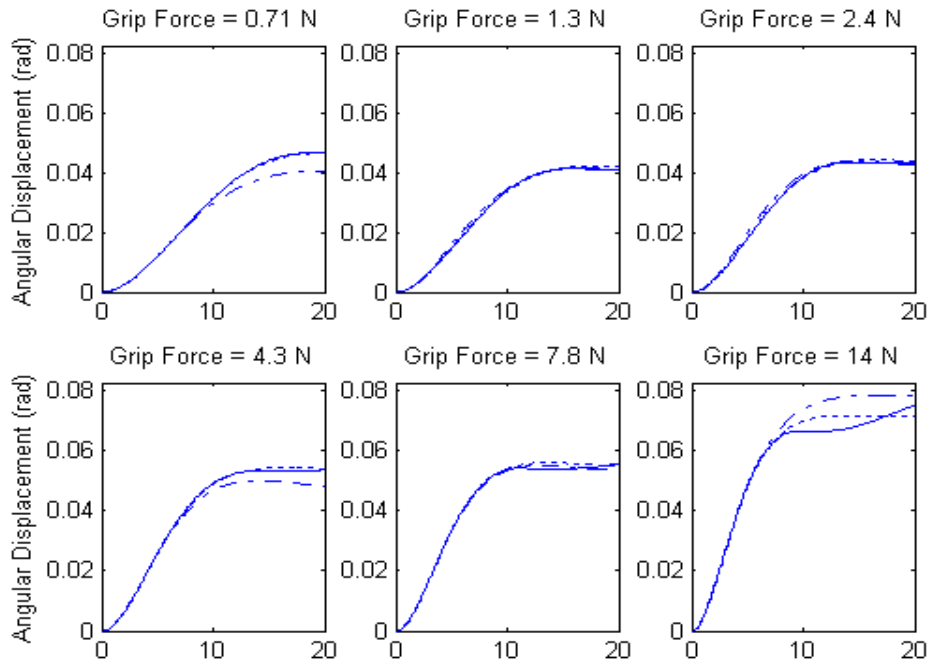


Figure 6: Measured step responses for a trial at six different grip forces (solid lines), simulated trajectories based on model estimates derived from the same data (dotted lines), and simulated trajectories based on models derived using data from a different trial (dot-dashed lines).

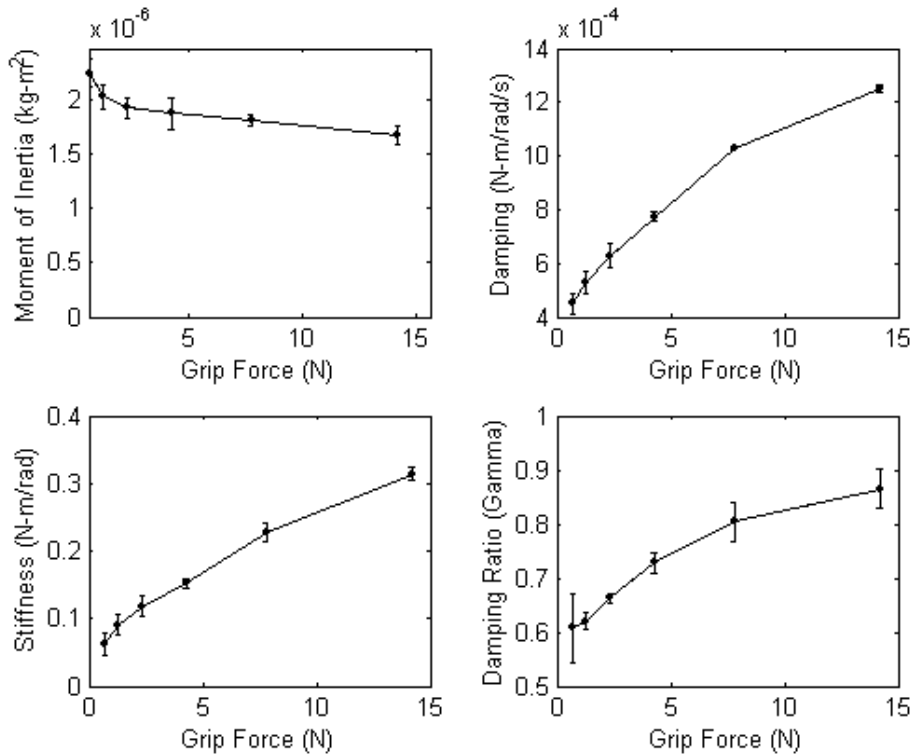


Figure 7: Moment of Inertia, Damping, Stiffness, and Damping Ratio for One Subject

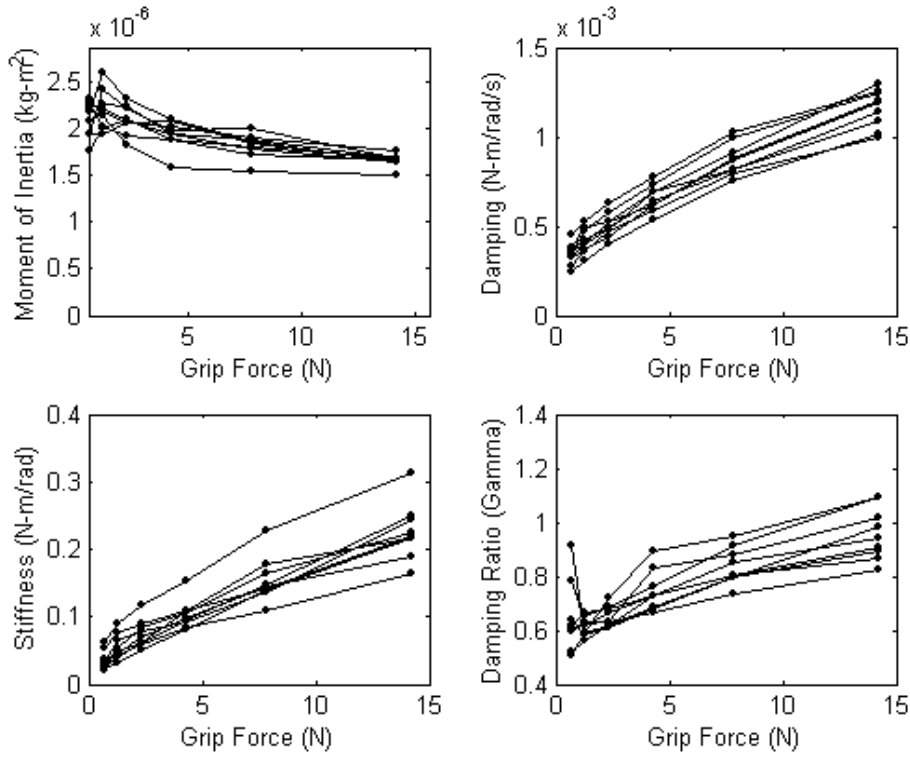


Figure 8: Moment of Inertia, Damping, Stiffness, and Damping Ratio for All Subjects

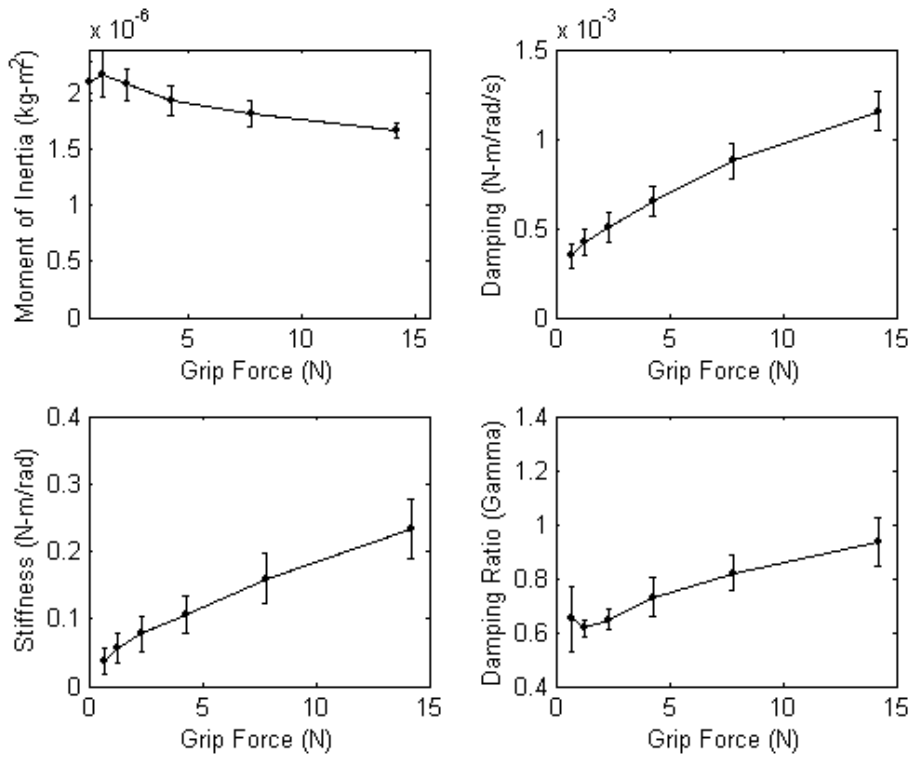


Figure 9: Moment of Inertia, Damping, Stiffness, and Damping Ratio Averaged Across All Subjects